Stable and unstable development of an interfacial sliding instability

Robert C. Viesca
Department of Civil and Environmental Engineering, Tufts University, Medford, MA 02155 USA
(Dated: June 3, 2016)

Examining a nonlinear instability of sliding rate on a frictional interface of elastic bodies, we investigate whether lab-constrained frictional relations suggest universal scaling under even the simplest of configurations. We find blow-up solutions by solving an equivalent, classical problem in fracture mechanics. The solutions are fixed points of a dynamical system and we show that their stability is lost by a cascade of Hopf bifurcations as a single problem parameter is increased, leading to chaotic dynamics.

The interest in understanding interfacial friction and its role in stick-slip sequences stems from problems ranging from sliding of an object on a surface [1] to the seismic cycle of tectonic faults [2, 3]. The elasticity of these bodies in contact permits differential slip along the interface. With sufficient compliance, stick-slip behavior may emerge as the result of the nucleation, fast propagation, and arrest of a shear rupture on the interface. Laboratory observations of sliding friction show a dependence on slip rate and its history, or state, and form the basis of a phenomenological model of friction [4, 5]. When the steady-state dependence is rate weakening, slip instabilities, characterized by a diverging slip rate, may emerge at the interface between elastic bodies [6, 7]. This divergence is limited by the bodies' inertia and these instabilities are thought, for example, to nucleate the fast rupture transition from stick to slip, including earthquake-generating dynamic rupture on geologic faults [8].

How does elasticity of the bodies couple with friction at the interface to generate the local instability that nucleates the rupture transition? Here we examine how an instability develops under a model for sliding friction for a wide range of material interfaces. Focusing on the nonlinear stages of the instability, we find that its development is in common with an array of seemingly disparate finite-time instabilities [9]. These include problems of reaction-diffusion [10], fluid dynamics [11, 12], and aggregation [13, 14]. Such instabilities show universal scaling, in which quantities diverge or shrink with a characteristic scaling in time and self-similar distribution in space that are both independent of the external forcing or initial conditions that provoke the instability. Novel features of the frictional instability here are (i) an unprecedented transition by which this universal behavior may be lost and replaced instead by an instability development that is, on the contrary, extremely sensitive to initial conditions and the manner of forcing and (ii) that such an instability arises in linearly elastic systems, in which nonlinearity is introduced only in the frictional description.

A point of interest in model representations of the seismic cycle of rupture, arrest, and re-rupture has been whether spatiotemporal complexity may emerge in the stick-slip sequence purely from the coupling of elasticity with friction [2, 3, 15]. Here we focus on the stage of the cycle in which instability develops quasi-statically, before the slip rate's local divergence is limited by inertia and dynamic rupture is nucleated. Prior examinations of frictional instabilities have indicated that both universal or more complex behavior may be possible at this stage [16–18]; however, a coherent description of the asymptotic development of the nonlinear instability is lacking. Such a description is desirable to understand the behavior leading to earthquake initiation and its contribution to cycle complexity: is there a universal scaling to or more chaotic behavior of the preseismic acceleration of a fault towards dynamic rupture?

The coefficient of friction on an interface is presumed to depend on a state variable θ and the instantaneous sliding rate V [4, 5]. A representation of θ may be a weighted average of the recent history of slip-rate or its inverse (slowness); presuming memory fades over an amount of slip D_c (e.g., determined by a characteristic lengthscale of the interface, such as asperity size), one possible definition of θ is an exponentially decaying weighting of the slowness, which implies its evolution follows [5]

$$\frac{\partial \theta}{\partial t} = 1 - \frac{V\theta}{D_c} \tag{1}$$

This form of the state variable and its evolution is commonly referred to as the aging-law, as at stationary contact, θ increases proportionally with contact time.

A proposed expression [5] for the friction coefficient f depending on θ and the instantaneous slip rate V that is consistent with experimental observations is

$$f = f_i + a\ln(V/V_i) + b\ln(V_i\theta/D_c) \tag{2}$$

where f_i and V_i are reference values of friction coefficient and sliding rate. The dimensionless coefficients a and b determine the magnitude of the direct and evolutionary responses to changes in slip rate implied in the terms that the coefficients precede. While the direct effect is physically motivated in terms of a creep process acting at asperity contacts, the apparent evolution effect is empirical [7]. When $a < b$, rate-weakening behavior is possible, and an interface sliding at a uniform rate is unstable to small perturbations [6, 7]. We look beyond

these initial stages of linear stability to understand the nonlinear development in the asymptotic limit of diverging slip rate.

For a frictional interface, the shear strength $\tau_s = \sigma f$, where σ is the surface-normal stress. The shear stress on the interface may be expressed as $\tau = \tau_o + \tau_{el}$, where τ_o is the shear stress that would be resolved on the interface if it were locked (e.g., due to an external loading) and τ_{el} is the shear stress change due to a distribution of interfacial slip δ. For quasi-static sliding, we may generally write $\tau_{el} = \mathcal{L}(\delta)$ where $\mathcal{L}$ is a functional whose form depends on the mode of slip and the elastic configuration (e.g., two half-spaces in contact, or a layer sliding above a substrate) and operates on the instantaneous distribution of slip and not its history. The interaction due to $\mathcal{L}$ may be local or non-local. $\mathcal{L}$ has the properties that $\partial\tau_{el}/\partial t = \mathcal{L}(V)$ and that $\mathcal{L}[g(t)h(\mathbf{x})] = g(t)\mathcal{L}[h(\mathbf{x})]$. When and where sliding on the interface occurs, $\tau = \tau_s$. Consequently,

$$\sigma\frac{\partial f}{\partial t} = \frac{\partial \tau_o}{\partial t} + \mathcal{L}(V) \tag{3}$$

Using a change of variables we look for solutions that correspond to a sliding instability, in which slip rate diverges in finite time. We transform t to a new variable s with the relation $ds/dt = 1/t_f(t)$ where $t_f(t) = t_{in} - t$ is the time from instability: as $t \to t_{in}$, $s \to \infty$. In place of considering V, we consider the variable W defined implicitly by $V(\mathbf{x},t) = W[\mathbf{x}, s(t)]D_c/t_f(t)$. Lastly, in place of θ, we consider the variable $\Phi[\mathbf{x}, s(t)] = 1 - D_c/[V(\mathbf{x},t)\theta(\mathbf{x},t)]$, which provides information on the proximity to steady-state sliding, occurring when $\Phi = 0$. The first two changes are suggested by scaling considerations [19], the last by our choice of the state evolution law. Understanding the behavior of W and Φ in the limit $s \to \infty$ informs on the manner of instability development.

The change leads to the new pair of evolution equations

$$\begin{aligned}\frac{\partial W}{\partial s} &= W\frac{b}{a}\tilde{\mathcal{L}}(W) + \frac{b}{a}W^2\Phi - W \\ \frac{\partial \Phi}{\partial s} &= (1-\Phi)\left[\frac{b}{a}\tilde{\mathcal{L}}(W) + \left(\frac{b}{a} - 1\right)W\Phi\right]\end{aligned} \tag{4}$$

with the non-dimensional operator $\tilde{\mathcal{L}} = (D_c/\sigma b)\mathcal{L}$. There is a single problem parameter, a/b, limited to $0 < a/b < 1$ for rate-weakening behavior. In arriving to (4), we acknowledged that τ_o is negligible in (3) if slip rate diverges, leading to autonomous evolution equations for V and θ (and, similarly, W and Φ).

Fixed-points of the dynamical system (4) are $W = \mathcal{W}(\mathbf{x})$, $\Phi = \mathcal{P}(\mathbf{x})$, which correspond to a slip rate diverging with a fixed distribution and proximity to steady-state sliding. From (4), we find that fixed points satisfy

$$\left(1 - \frac{a}{b}\right) + \tilde{\mathcal{L}}(\mathcal{W}) = \begin{cases} 1 - \mathcal{W} & \mathcal{W} \le 1 \\ 0 & \mathcal{W} \ge 1 \end{cases} \tag{5}$$

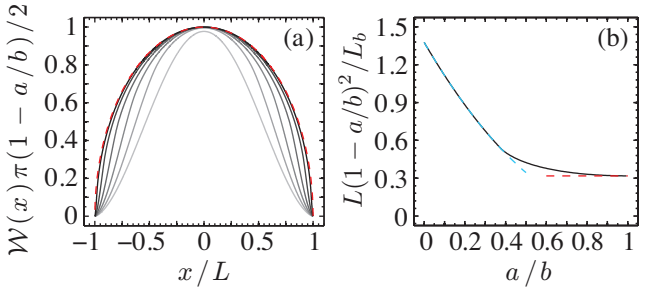

FIG. 1. For in-plane or anti-plane slip between elastic halfspaces, fixed points of (4) correspond to a diverging slip rate with spatial distribution $\mathcal{W}$ (a) of half-length L (b), which depend on the problem parameter a/b. Dashed lines show asymptotic behavior (see text). Progressively dark curves in (a) correspond to solutions for a/b of $0.3781..., 0.5, 0.6, ..., 0.9$.

where $\mathcal{W}$ is compact and vanishes on its boundary and with $\mathcal{P} = 1$ where $\mathcal{W} \le 1$ and $\mathcal{P} = 1/\mathcal{W}$ where $\mathcal{W} \ge 1$. These last conditions on $\mathcal{P}$ follow from (4) and given that $\Phi \le 1$ by definition. Remarkably, the problem (5) of solving for $\mathcal{W}$ is equivalent to a form of the classical cohesive crack problem in fracture mechanics [20, 21]: solving for the slip distribution of a crack whose strength weakens linearly from a peak strength τ_p to a residual level τ_r over a characterisic slip δ_c and is in equilibrium with a uniform background stress τ_b, or

$$\tau_b + \mathcal{L}(\delta) = \begin{cases} \tau_p - (\tau_p - \tau_r)\delta/\delta_c & \delta \le \delta_c \\ \tau_r & \delta \ge \delta_c \end{cases} \tag{6}$$

The similarity between (5) and (6) implies that the stress changes and slip increments during an instability developing in the manner of the fixed-point resemble the distributions of stress and slip of a slip-weakening fracture.

Whether these fixed points are attractive and asymptotically stable is determined by a linear stability analysis. We examine the evolution of small perturbations from the fixed point in the form $\Phi(x,s) = \mathcal{P}(x) + \epsilon\phi(x)\exp(\lambda s)$, $W(x,s) = \mathcal{W}(x) + \epsilon\omega(x)\exp(\lambda s)$. Following substitution in (4) and keeping terms of $O(\epsilon)$, we arrive to an eigenvalue problem for eigenvalues λ and eigenmodes ω and ϕ (Appendix). Two eigenvalues and eigenmodes may be anticipated and correspond to translational symmetry in space and time [22]: respectively, $\lambda = 0$, $\lambda = 1$. The real part of the remaining eigenvalues determines the fixed point stability.

We apply these results to a particular elastic configuration and modes of quasi-static slip: in-plane (mode-II) or anti-plane (mode-III) slip between two elastic halfspaces. Here, $\mathbf{x}$ is the single spatial dimension x along which variations occur, and the operator $\mathcal{L}$ takes the form [23]

$$\mathcal{L}(V) = \frac{\mu'}{2\pi}\int_{-L_-}^{L_+}\frac{\partial V/\partial x'}{x' - x}dx' \tag{7}$$

where L_+ and L_- are the endpoints of the slipping area, and the effective shear modulus μ' is the shear modulus μ in mode III and $\mu/(1-\nu)$ in mode II, with Poisson ratio ν. When solving for $\mathcal{W}$, the problem symmetry implies $L_+ = L_- = L$. The length $L_b = \mu' D_c/(\sigma b)$ emerges as a characteristic length scale for spatial variations.

Elasticity provides interactions between points on the sliding surface, which may range between the non-local interaction implied by (7) to a local interaction in which $\mathcal{L}$ is a derivative. In the Supplementary Materials [24] we consider slip on a surface near a boundary and show that the non-local interaction (7) transitions to a local one as a parameter comparing the distance to the free boundary h to the lengthscale L_b is reduced. We find that the results to follow for the particular configuration embodied by (7) are generally independent of the range of interaction.

We numerically solve the problem of finding the fixed points satisfying (5) with (7): i.e., finding $\mathcal{W}$ (Figure 1a), L (Figure 1b), and, implicitly, $\mathcal{P}$ as a/b is varied. We retrieve end-member scalings for L: $L = (1.3774...)L_b$ for $0 < a/b < (0.3781...)$ and $L = L_b/[\pi(1-a/b)^2]$ as $a/b \to 1$. These scalings were first suggested by prior analysis and numerical solutions [17]: the value of L for the small values of a/b was found when looking for separable blow-up solutions limited to $\Phi = 1$ within $|x| \le L$; and the latter was inferred using a small-scale-yielding argument based on results of numerical solutions of the original system of evolution equations resulting from (1) and (2) with (3). Here we retrieve the former scaling as a special case and find a stronger argument for the latter scaling owing to the equivalence of the problem of finding $\mathcal{W}$, $\mathcal{P}$ to solving a classical fracture problem in which a small-scale-yielding analysis is appropriate in the limit $a/b \to 1$. In this limit, $\mathcal{W}$ converges to the elliptic solution $\mathcal{W}(x) = \sqrt{1-(x/L)^2}/[(1-a/b)\pi/2]$.

To perform the linear stability analysis of the fixed points for this configuration for a given value of a/b, we numerically solve the associated eigenvalue problem. We find that fixed points are asymptotically stable for $0 < a/b < (0.3781...)$: i.e., eigenvalues not associated with translational symmetries have negative real parts. Asymptotic stability is first lost as a/b is increased beyond this range by an eigenvalue translating along the real axis and whose eigenmode is an odd function. As a/b is increased further, subsequent modes become unstable through an apparently infinite succession of Hopf bifurcations as $a/b \to 1$. Fig. 2 shows the trajectory of the complex eigenvalues of the first six modes to undergo a Hopf bifurcation.

The cascade of Hopf bifurcations implies the slip instability develops chaotically beyond a threshold value of a/b. For a system whose fixed point first loses stability by a supercritical Hopf bifurcation, the asymptotic behavior is a limit cycle. A second Hopf bifurcation would imply oscillations with an additional frequency leading to a limit torus; incommensurate frequencies result in quasi-periodic behavior. The continued sequence would suggest an accumulation of unstable modes and mirrors a proposed route to turbulent, chaotic fluid flow [25, 26], in which such a cascade occurs as viscosity $\eta \to 0$. However, many unstable modes may be unnecessary for chaotic behavior since prior work [27, 28] indicates that, following a third Hopf bifurcation, the expected quasi-periodic limit torus is not stable to perturbations and may be replaced by a strange attractor.

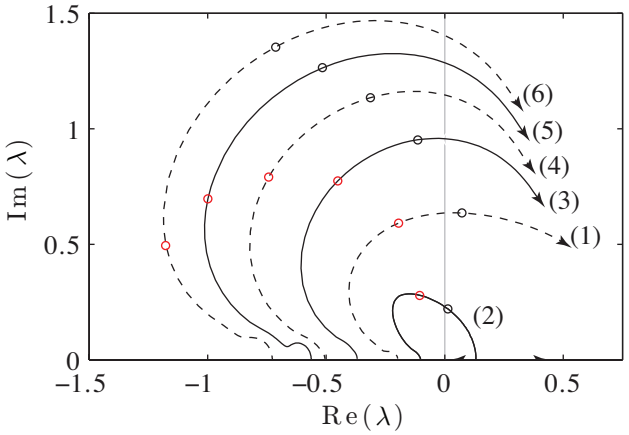

FIG. 2. Eigenvalue trajectories as a/b is increased. The first six Hopf-bifurcating eigenvalues to cross the imaginary axis are shown (order indicated). Solid and dashed lines indicate the corresponding eigenmode is even and odd, respectively. Red and black circles indicate eigenvalue positions when $a/b = 0.65$ and 0.75, respectively. The final position of each trajectory corresponds to a value of a/b of 0.92 for the left branch of innermost trajectory, and 0.98 for all others.

The dramatic loss of fixed-point stability as $a/b \to 1$ follows the approach of the fixed-point behavior towards steady-state slip. In this limit, $\mathcal{P} \to 0$ nearly everywhere on $|x| \le L$, except within a boundary layer near $|x| = L$ whose length is comparable to L_b: the behavior in this limit is one of diverging velocity under steady-state sliding. Uniform, steady-state sliding is known to be unstable perturbations with a wavelength exceeding $\lambda_{cr} \sim L_b/(1-a/b)$ [6, 7]. Here, L exceeds λ_{cr} for a/b near 1 since $L \sim L_b/(1-a/b)^2$.

To compare against the fixed-point stability analysis, we find numerical solutions to the evolution equations for slip rate and state, (1) and (2) with (3) and (7), and examine the asymptotic development of a slip instability. The slipping region is the entire real line: i.e., $L_\pm \to \pm\infty$ in (7). Initially, the surface uniformly slides at steady-state. A perturbation is applied at $t = 0$ and induces an instability. The perturbation is a slowly increasing external forcing τ_o, spatially compact and symmetric. With symmetry imposed, the loss of fixed-point stability occurs only through a series of Hopf bifurcations and the fixed points are asymptotically stable up to $a/b \approx 0.74$,

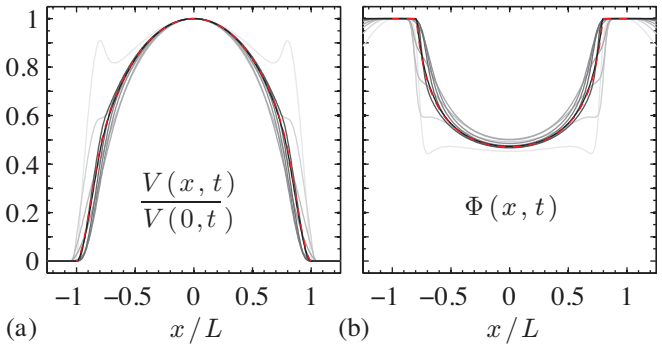

FIG. 3. Numerical solution (greyscale lines) for slip rate- and state-evolution for $a/b = 0.7$ for a surface perturbed from steady-state showing snapshots in time of the spatial distributions along the surface dimension x of (a) scaled, diverging slip rate and (b) the distance from steady state slip Φ. Increasing greyscale corresponds to increasing progression of instability. Distance x is scaled by the value of L that corresponds to $a/b = 0.7$ for comparison with the fixed point. Solution shows expected asymptotic convergence towards fixed point distributions $\mathcal{W}(x)/\mathcal{W}(0)$ and $\mathcal{P}(x)$ (red-dashed lines).

where the first even-mode Hopf bifurcation occurs. We examine a case where the problem parameter $a/b = 0.7$ (Fig. 3). While sliding occurs along the real line, we find that the blowup of slip rate asymptotes to the compact distribution of the fixed point solution.

We show the changing character in the instability development as a/b increases past the sequence of even-mode Hopf bifurcation thresholds (Fig. 4). We use slip at a point as a proxy for the independent variable s: for a slip rate that diverges in the manner of the fixed points, the two are linearly related. Following the first Hopf bifurcation, asymptotic convergence is replaced by a finite-amplitude limit cycle, which in turn gives way following the second Hopf bifurcation (at $a/b \approx 0.79$) to aperiodic oscillations with similar amplitude and two dominant, incommensurate frequencies showing nearly quasi-periodic behavior. After the third Hopf bifurcation (occuring at $a/b \approx 0.87$), there are three unstable eigenmodes. The eigenvalue of one of these modes loses its imaginary part at $a/b \approx 0.86$ after the complex conjugate eigenvalue pair coalesces on the real line and follows opposing trajectories (Fig. 3). Notwithstanding, the resulting development of the instability is noticeably aperiodic.

The material parameter a/b leading to chaotic behavior here is distinct from a parameter derived from external forcing. An example of the latter is the transition to a chaotic drip sequence with an increase of a faucet's fluid flow [29–31]. The former implies chaotic behavior is inherent to the system, independent of the manner of external forcing or its strength, provided only the forcing is sufficient to provoke instability.

In seismic cycle models with rate- and state-dependent friction, spatiotemporal complexity is often notably absent and seismic cycles are periodic. However, frequently in these models $a/b \leq 0.8$, where we find slip instability (and hence, earthquake nucleation) does not develop chaotically but in a universal manner consistent with the observed periodicity. The exploration of a potentially relevant and interesting range of parameter space may be limited owing to computational considerations (due to the disparity of lengths L and L_b); however, sensitive dependence of instability development on pre-instability conditions may lead to marked differences in the nucleation phase from one event to the next and not the erased memory of ad hoc initial conditions frequently seen.

Experimental observation of interfacial rupture via changes in contact area or photographically observed deformation provide insight into the spatiotemporal evolution of unstable interfacial slip. This includes dynamic rupture events and their arrest [1, 32–34], and the quasi-static nucleation phase preceding dynamic rupture [35, 36]. In part aiming to reproduce the latter experimental observations, numerical solutions of the evolution equations for slip rate and state for the friction law considered here show that the nucleation of dynamic rupture is preceded by a quasi-static, crack-like propagation of accelerating slip rate [17, 37]. The results here provide an interpretation of such crack-like growth as the attraction of the slip rate to towards the fixed point: the propagation of these crack-like events occurs towards lengths consistent with the values of L found here, and the crack-like slip-rate profiles resemble a fundamental mode of ω from the linear stability analysis.

The results provide several testable predictions amenable to the above experiments. The foremost is the possibility of confirming the universal scaling of the acceleration of slip towards the nucleation of a dynamic rupture: i.e., a scaling independent of the forcing or initial conditions. Comparing the slip rate to its acceleration, the fixed-point solutions suggest the asymptotic scaling $V/(\partial V/\partial t) = t_f$. Experimentally this requires a high-frequency measurement of displacement rate at a point on the interface where an instability emerges. A distribution of such measurements or a proxy for the extent of slip (e.g., such as the evolution of contact area), may also reveal whether the instability is attracted to develop over a characteristic length L and distribution $\mathcal{W}$. Prior experimental studies [1, 32–36, 38] have made such measurements. However, either the scaling of sliding rate divergence was not a consideration; the sampling rate was during the quasi-static acceleration insufficient to discriminate a scaling; or the focus of measurement was on rupture events on the scales much larger than the nucleating instability. Furthermore, whereas observations on the larger scale are well represented by a shear rupture with small-scale-yielding [33, 34, 39], in which details of frictional evolution are implicitly neglected, the results here suggest that examination of the nucleating instability may serve as a better diagnostic of the manner

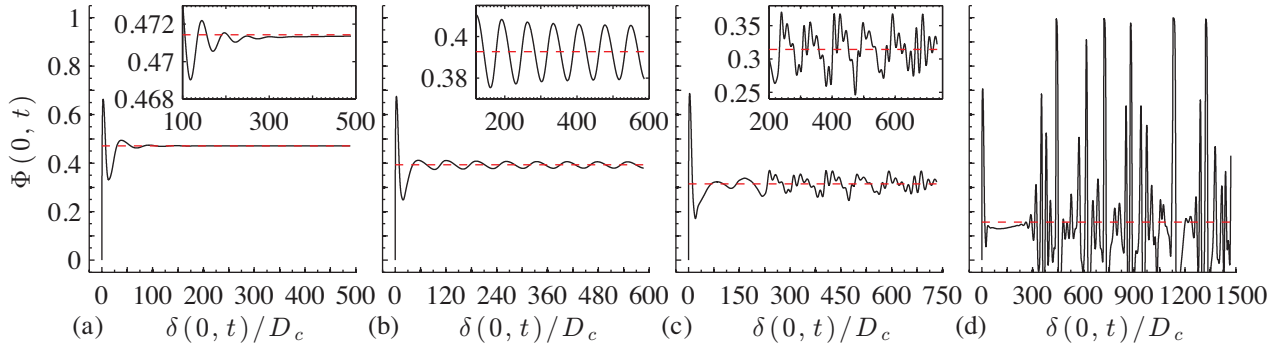

FIG. 4. Four numerical solutions to slip rate- and state evolution equations for a surface perturbed from steady-state for select values of the problem parameter a/b: (a) 0.7 (b) 0.75 (c) 0.8 (d) 0.9. Hopf bifurcations occur at values of a/b between those of the solutions presented here (see text). The history of one solution variable Φ at a single point on the surface with slip at the same point is shown for each value of a/b. As a/b is increased we find asymptotic convergence in the case of (a) is replaced by a limit cycle following the first Hopf bifurcation in (b) and nearly quasi-periodic behavior with two dominant frequencies following the second Hopf bifurcation in (c), in turn followed by aperiodic behavior in (d) after the third Hopf bifurcation. The corresponding fixed-point value of Φ at each value of a/b is indicated by a red-dashed line.

of frictional evolution.

To aid such diagnostic comparisons, there are several indications the asymptotic analysis pursued here may be fruitfully applied to understand instability development under other evolution laws for state, θ, as well as altogether different formulations for the rate and state dependence of friction. We highlight in the Supplementary Materials [24] another experimentally motivated state evolution law [40, 41] that also admits self-similar blow-up solutions whose form are analogous to those determined by (5). These solutions are consistent with numerical solutions to evolution equations [42, 43]. Furthermore, a preliminary examination of nonlinear instability development in numerical solutions [44] of a recently proposed frictional description [45] shows indications for its occurrence as fixed-point attraction [24].

R.C.V. acknowledges support from the National Science Foundation (grant EAR-1344993), and is grateful to the Équipe Tectonique et Mécanique de la Lithosphère at the Institut de Physique du Globe de Paris for their hospitality, and to Shmuel M. Rubinstein for providing comments on a draft of the manuscript.

APPENDIX

Linear stability analysis. To determine the linear stability of the fixed points we examined the evolution of perturbations to the fixed points of the form

$$W(\boldsymbol{x}, s) = \mathcal{W}(\boldsymbol{x}) + \epsilon\omega(\mathbf{x})e^{\lambda s}$$
$$\Phi(\boldsymbol{x}, s) = \mathcal{P}(\boldsymbol{x}) + \epsilon\phi(\mathbf{x})e^{\lambda s}$$

Substituting the above into the dynamical system (4), we arrive to an eigenvalue problem of the form

$$\lambda\omega = \mathcal{A}(\omega, \phi)$$
$$\lambda\phi = \mathcal{B}(\omega, \phi)$$

for which the eigenmodes $\omega(\mathbf{x})$ and $\phi(\mathbf{x})$ and eigenvalues λ are to be solved. The functional operators $\mathcal{A}$ and $\mathcal{B}$ are linear in their arguments,

$$\mathcal{A}(\omega, \phi) = \frac{b}{a}\mathcal{W}\left[\omega\mathcal{P} + \mathcal{L}(\omega)\right] + \frac{b}{a}\mathcal{W}^2\phi$$
$$\mathcal{B}(\omega, \phi) = -\phi\left[1 - \mathcal{W}\mathcal{P}\right] + \left[1 - \mathcal{P}\right]\left[\frac{b}{a}\mathcal{L}(\omega) + \left(\frac{b}{a} - 1\right)\left(\omega\mathcal{P} + \mathcal{W}\phi\right)\right]$$

Given the operator $\mathcal{L}$, which depends on the elastic configuration, the functions $\mathcal{W}$ and $\mathcal{P}$ are provided by solution of the fixed-point equation (5). We recall that $\mathcal{W}$ and $\mathcal{P}$ depend on a/b.

When $\mathcal{L}$ is given by (7), the operator is discretized assuming ω is piecewise constant over regular intervals within $|x| \leq L$. $\mathcal{W}$, $\mathcal{P}$, and ϕ are likewise discretized at those intervals. The eigenvalue problem reduces to one of a linear matrix. Numerically solving this problem for various values of a/b, we find that the trajectories of the complex eigenvalues yield an apparently infinite sequence of Hopf bifurcations as $a/b \to 1$. In Fig. 3 we show the trajectories of the first six modes to bifurcation. The sequence of values of a/b at which these first six bifurcations occur are approximately: 0.72, 0.74, 0.79, 0.84, 0.87, and 0.91.

[1] S. M. Rubinstein, G. Cohen, and J. Fineberg, Nature **430**, 1005 (2004).

[2] R. Burridge and L. Knopoff, B. Seismol. Soc. Am. **57**, 341 (1967).
[3] J. R. Rice, J. Geophys. Res. **98**, 9885 (1993).
[4] J. H. Dieterich, J. Geophys. Res. **84**, 2161 (1979).
[5] A. Ruina, J. Geophys. Res. **88**, 10359 (1983).
[6] J. R. Rice and A. L. Ruina, J. Appl. Mech. **50**, 343 (1983).
[7] See, for example, the discussion of J. R. Rice, N. Lapusta, and K. Ranjith, J. Mech. Phys. Solids **49**, 1865 (2001).
[8] S. T. Tse and J. R. Rice, J. Geophys. Res. **91**, 9452 (1986).
[9] In addition to references to follow, for further discussion and examples see also J. Eggers and M. A. Fontelos, Nonlinearity **22**, R1 (2009) and *Singularities: Formation, Structure, and Propagation*, Cambridge Texts in Applied Mathematics (Cambridge University Press, Cambridge, 2015).
[10] Y. Giga and R. V. Kohn, Commun. Pur. Appl. Math **38**, 297 (1985).
[11] J. Eggers, Phys. Rev. Lett. **71**, 3458 (1993).
[12] A. L. Bertozzi, M. P. Brenner, T. F. Dupont, and L. P. Kadanoff, in *Trends and Perspectives in Applied Mathematics*, edited by L. Sirovich, F. John, and J. E. Marsden (Series: Applied mathematical sciences, Springer-Verlag, New York, 1994) pp. 155–208.
[13] H. G. Othmer and A. Stevens, SIAM J. Appl. Math. **57**, 1044 (1997).
[14] M. P. Brenner, P. Constantin, L. P. Kadanoff, A. Schenkel, and S. C. Venkataramani, Nonlinearity **12**, 1071 (1999).
[15] J. M. Carlson and J. S. Langer, Phys. Rev. Lett. **62**, 2632 (1989).
[16] J. H. Dieterich, Tectonophysics **211**, 115 (1992).
[17] A. M. Rubin and J.-P. Ampuero, J. Geophys. Res. **110**, B11312 (2005).
[18] J.-P. Ampuero and A. M. Rubin, J. Geophys. Res. **113**, B01302 (2008).
[19] G. I. Barenblatt, *Scaling, self-similarity, and intermediate asymptotics* (Cambridge University Press, Cambridge, 1996).
[20] D. S. Dugdale, J. Mech. Phys. Solids **8**, 100 (1960).
[21] G. I. Barenblatt, in *Advances in Applied Mechanics Volume 7* (Elsevier, 1962) pp. 55–129.
[22] A. J. Bernoff, A. L. Bertozzi, and T. P. Witelski, J. Stat. Phys. **93**, 725 (1998).
[23] J. R. Rice, in *Fracture*, edited by H. Liebowitz (Fracture: an advanced treatise, New York, 1968) pp. 192–311.
[24] See Supplemental Material at [url] for brief discussions concerning local and non-local elastic interactions; fixed points and their stability under local interactions; and other descriptions of state or frictional evolution.
[25] L. D. Landau, Dokl. Akad. Nauk SSSR **44**, 939 (1944) and see also L. D. Landau and E. M. Lifshitz, *Fluid Mechanics*, Vol. 6 (Pergamon Press, 1987).
[26] E. Hopf, Commun. Appl. Math **1**, 303 (1948).
[27] D. Ruelle and F. Takens, Commun. Math. Phys. **20**, 167 (1971).
[28] S. Newhouse, D. Ruelle, and F. Takens, Commun. Math. Phys. **64**, 35 (1978).
[29] R. Shaw, "The dripping faucet as a model chaotic system," Aerial Press (1984).
[30] P. Martien, S. C. Pope, P. L. Scott, and R. S. Shaw, Phys. Lett. A **110**, 399 (1985).
[31] P. Coullet, L. Mahadevan, and C. S. Riera, J. Fluid Mech. **526**, 1 (2005).
[32] O. Ben-David, S. M. Rubinstein, and J. Fineberg, Nature **463**, 76 (2010).
[33] I. Svetlizky and J. Fineberg, Nature **509**, 205 (2014).
[34] E. Bayart, I. Svetlizky, and J. Fineberg, Nat. Phys. , 1 (2015).
[35] S. Nielsen, J. Taddeucci, and S. Vinciguerra, Geophys. J. Int. **180**, 697 (2010).
[36] S. Latour, A. Schubnel, S. Nielsen, R. Madariaga, and S. Vinciguerra, Geophys. Res. Lett. **40**, 5064 (2013).
[37] Y. Kaneko and J.-P. Ampuero, Geophys. Res. Lett. **38** (2011).
[38] M. Ohnaka and L. F. Shen, J. Geophys. Res. **104**, 817 (1999).
[39] D. S. Kammer, M. Radiguet, J.-P. Ampuero, and J.-F. Molinari, Tribology Letters **57** (2015).
[40] K. Nagata, M. Nakatani, and S. Yoshida, J. Geophys. Res. **117**, B02314 (2012).
[41] P. Bhattacharya, A. M. Rubin, E. Bayart, S. H. M, and M. C, J. Geophys. Res. **120**, 6365 (2015).
[42] N. Kame, S. Fujita, M. Nakatani, and T. Kusakabe, Pure Appl. Geophys. **172**, 2237 (2013).
[43] P. Bhattacharya and A. M. Rubin, J. Geophys. Res. **119**, 2272 (2014).
[44] Y. Bar-Sinai, R. Spatschek, E. A. Brener, and E. Bouchbinder, Phys. Rev. E **88**, 060403 (2013).
[45] E. Bouchbinder, E. A. Brener, I. Barel, and M. Urbakh, Phys. Rev. Lett. **107**, 235501 (2011).